ACS MATERIALS Au
AN OPEN ACCESS JOURNAL OF THE AMERICAN CHEMICAL SOCIETY

pubs.acs.org/materialsau

Article

Impact of the Cationic Moiety of Ionic Liquids on Chemoselective Artificial Olfaction

Ana Rita Oliveira, Efthymia Ramou, Susana I. C. J. Palma, Carina Esteves, Arménio Barbosa, and Ana Cecília Afonso Roque*

Cite This: https://doi.org/10.1021/acsmaterialsau.3c00042

Read Online

ACCESS | Metrics & More | Article Recommendations | Supporting Information

ABSTRACT: Ionogels and derived materials are assemblies of polymers and ionic liquids characterized by high stability and ionic conductivity, making them interesting choices as gas sensors. In this work, we assessed the effect of the ionic liquid moiety to generate ionogels and hybrid gels as electrical and optical gas sensors. Six ionic liquids consisting of a constant anion (chloride) and distinct cationic head groups were used to generate ionogels and hybrid gels and further tested as gas sensors in customized electronic nose devices. In general, ionogel-based sensors yielded higher classification accuracies of standard volatile organic compounds when compared to hybrid material-based sensors. In addition, the high chemical diversity of ionic liquids is further translated to a high functional diversity in analyte molecular recognition and sensing.

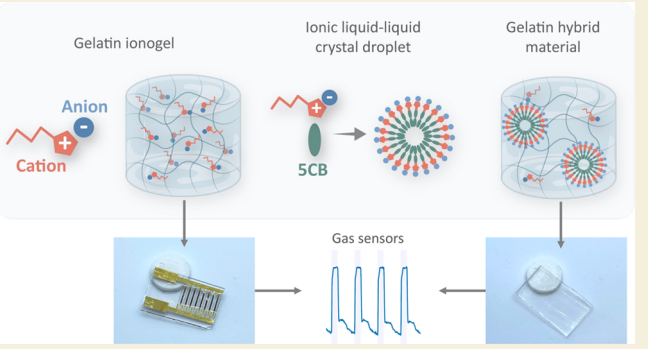

KEYWORDS: *electronic nose, gas sensing, hybrid gels, ionogels, ionic liquids*

INTRODUCTION

Ionic liquids (ILs) are organic salts that consist only of ions, a positive ion (cation) and a negative ion (anion) bound together via electrostatic interactions. Some important features of ILs include high electrochemical and thermal stability, negligible vapor pressure, and high ionic conductivity. One of the most attractive aspects of ILs is that their physicochemical properties can be tuned by modifying the anion−cation pair, leading to innumerable possible structures tailored for different applications. ILs can be immobilized in polymeric matrices, giving rise to ion-based materials as ionogels, which combine the properties of both the polymer matrix and the corresponding IL.[1] Ionogels are appealing to develop innovative functional materials applicable in a variety of fields, namely, agents for the removal of pollutants,[2] controlled reaction media,[3] antimicrobial gels,[3] or stimuli-responsive and conductive films and fibers.[4]

Several studies report the chemoselective gas-sensing potential of ILs[5−7] and especially ionogels[8,9] Typically, ionogel-based gas sensors yield a fast and reversible response when exposed to different VOCs, which is mainly attributed to changes in the ion mobility. The incorporation of other functional molecules in the ionogel matrix, for example, liquid crystal (LC) molecules, can endow the resulting gel with additional properties and features, leading to numerous possibilities in the design of new sensing hybrid materials and additional optical transduction mechanisms[10]

In past studies, the ability to tune the composition of ionogels and hybrid materials and the respective impact on the gas-sensing properties were reported, for instance, by changing the polymer,[11,12] ionic liquid,[8,11] and liquid crystal[13,14] components in the formulation. In this study, we focus on changing the cation of the ionic liquid and explore the potential of six chloride-based ILs with distinct cationic moieties to generate sensors for VOC discrimination. We produced gelatin-based ionogels, which yield an electrical signal, and hybrid materials (otherwise named hybrid gels here), which additionally have a liquid crystal (5CB) component and yield an optical signal. The chloride-based ILs studied were 1-butyl-1-methylpiperidinium (BMPip), 1-butyl-1-methylpyrrolidinium (BMPyrr), 1-butylpyridinium, 1-butyl-2-methylpyridinium, and 1-butyl-4-methylpyridinium (BuPy, Bu_2Pic, and Bu_4Pic, respectively), and 1-butyl-3-methylimidazolium (BMIM). The BMIM cation was chosen here as the control as it is already reported to yield gelatin-based ionogels and hybrid gels that generate both electrical and optical responses in the presence of gas analytes.[8,14−16] The 4-

Received: May 19, 2023
Revised: August 1, 2023
Accepted: August 2, 2023

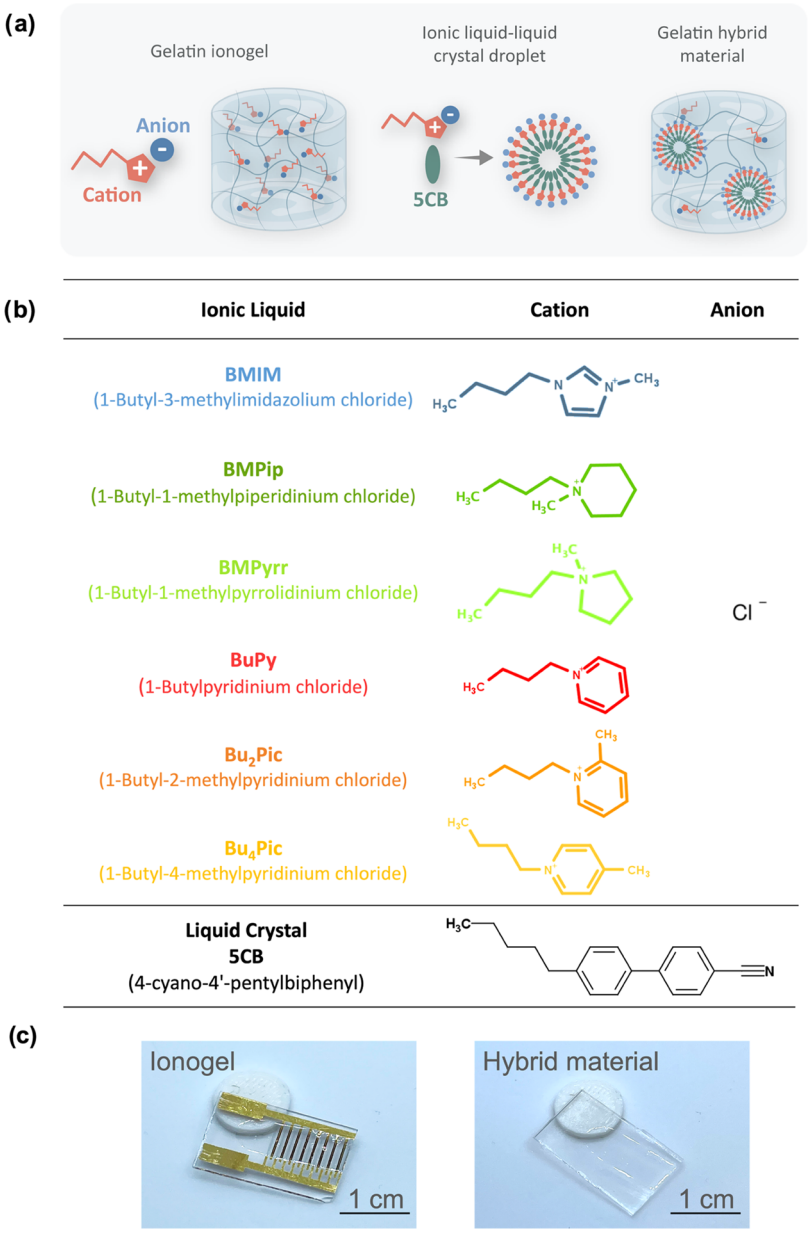

Figure 1. (a) Schematic representation of the materials used in this study. 5CB stands for the liquid crystal 4-cyano-4′-pentylbiphenyl. (b) Chemical structures of the six different ionic liquids and the liquid crystal used in this study. (c) Images displaying the gelatin ionogel and hybrid material used as electrical and optical gas sensors, respectively.

carbon chain of the cation was maintained constant, and when combined with the aromaticity of the cation, it contributed to low viscosity and high conductivity in IL materials,[17] and it is also a key element in the stabilization of self-assembled spherical interfaces encapsulating LC droplets.[18] The gas-sensing capabilities of the materials were tested in tailor-made electrical and optical electronic noses (e-noses), and the VOC classification capabilities were evaluated using an automatic classifier based on Support Vector Machines (SVM). We show that the production and use of sensing materials with distinct compositions and transduction mechanisms lead to increased selectivity and discrimination of different VOCs, which can be combined in an array to further advance the field of artificial olfaction.[19]

RESULTS AND DISCUSSION

In this work, chloride-based ionic liquids (ILs) with cationic groups from distinct families were evaluated to produce self-assembled gelatin materials (Figure 1). First, gelatin was dissolved and gelated with the studied ILs, yielding a set of six distinct ionogels. Second, adding the liquid crystal 4-cyano-4′-pentylbiphenyl (5CB) to the formulation yielded hybrid materials with compartmentalized droplets containing organized liquid crystal molecules.

The ionic conductivity of the IL component is maintained in ionogels. Typically, a threshold of 1 mS cm^{-1} is required in order to implement an IL-containing material into an electrical device.[20,21] Frequency-dependent ionic conductivity experiments performed for all ionogel formulations indicated that all of them act as ionic conductive materials, especially at 2000 Hz, which is the frequency at which the electrical e-nose

https://doi.org/10.1021/acsmaterialsau.3c00042
ACS Mater. Au XXXX, XXX, XXX−XXX

performs the measurements during the VOC discrimination assays (Figure 2a and Table S1). Above 103 Hz, the ionic

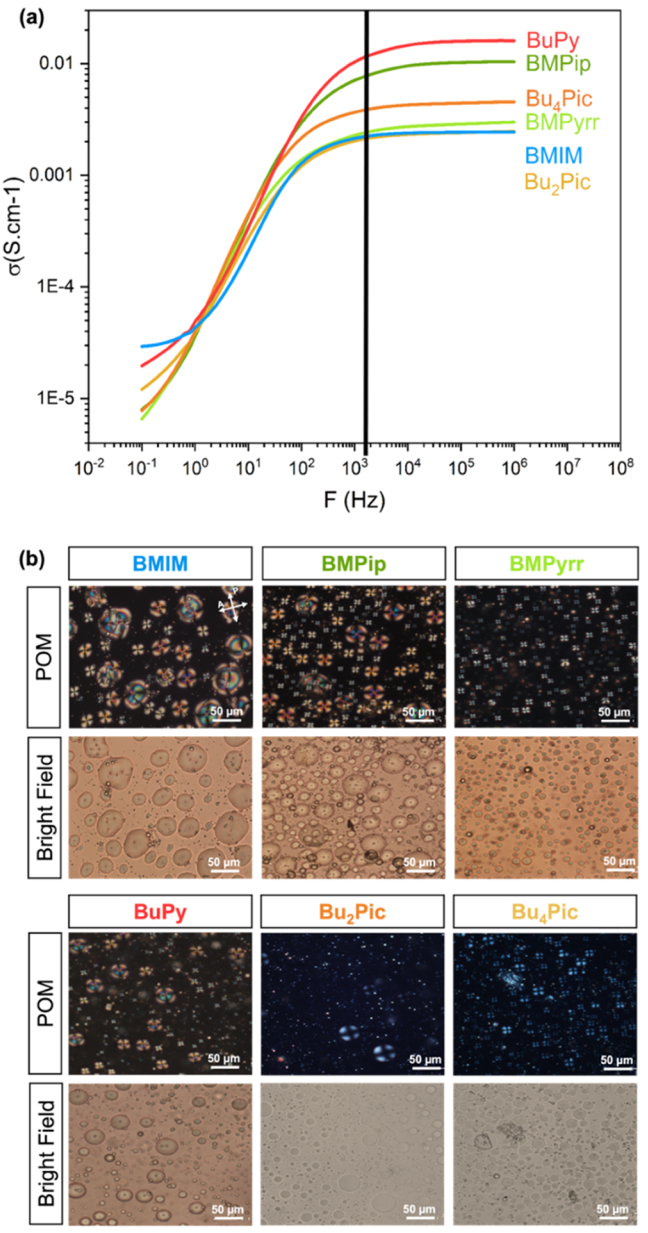

Figure 2. Characterization of the sensors produced in this work. (a) Conductivity results for all ionogels. The frequency at which the electrical e-nose performs the measurements during the experiments is represented by the black vertical line. (b) Morphological characterization of the optical hybrid material sensors through POM and bright-field images for BMIM, BMPip, BMPyrr, BuPy, Bu_2Pic, and Bu_4Pic sensors.

conductivity of the ionogels stabilizes. At 2 kHz, the conductivity values determined followed a decreasing order as follows: BuPy > BMPip > Bu_4Pic > BMPyrr > BMIM > Bu_2Pic. Cations containing aromatic moieties, such as those from pyridinium ILs, are known to make materials less viscous and therefore lead to great conductivity results[22]—an exception is observed for the Bu2Pic member of the pyridinium family and for BMIM from the imidazolium family. Bu_2Pic has a methyl group at the ortho position, conferring a more hydrophilic character to the IL (confirmed by the log *P* value; Table S1), which can explain its slightly different conductivity when compared to the remaining members of the pyridinium family.[23] In addition, the presence of a polymeric matrix can affect the conductivity of materials due to a less rigid entanglement of the ring within the polymer; therefore, the multicomponent assembly apparently leads to higher conductivity in the nonaromatic cation of the piperidium IL.[22] A similar justification can be given for the lower conductivity of the imidazolium IL, BMIM. These results are in accordance with the literature, where it is stated that the presence of rings—whether aromatic or cyclic—contributes to different viscosities in materials and therefore different ionic mobilities and ionic conductivities.[22,24,25] Also, it is known that the existence of methyl groups in the rings, placed in different positions, can also confer different hydrophobicities to the ILs.[23]

With regard to hybrid materials and considering the optical transduction mechanism occurring in the presence of IL−LC droplets, we started by studying the morphological aspects of all of the produced compositions via POM. In general, the gels present heterogeneous and polydispersed IL−LC droplets, which were stable over a week after production (Figure S2), and their topography can be traced at the surface of the materials (Figure S3). Hybrid gels containing BMIM and BMPip displayed the largest droplets over a wider range of diameters, but predominantly between 15−20 and 40−50 μm, respectively, followed by Bu_2Pic (5−15 μm), and finally BMPyrr, BuPy, and Bu_4Pic showed the smallest droplets (5−10 μm) (Figure S4). It was observed that the LC inside the droplets assumed a radial configuration, which is revealed by the Maltese cross pattern seen in POM images under crossed polarizers.[10] In bright-field images, the characteristic core defect, named hedgehog, can be seen. The radial director profile is due to the homeotropic alignment provided essentially by the interactions of the LC with the cation of the IL. The presence of the radial configuration of LCs is actually quite relevant as it is shown to provide a fast and dynamic optical response upon exposure to VOCs.[16]

Ionogels as VOC Electrical Sensors

In the electrical e-nose, films of ionogels spread on interdigitated electrodes are used as VOC sensors (Figure 1). When VOCs adsorb onto an ionogel sensor, there will be an increase or decrease in the mobility of the IL ions present in the gel composition due to interactions between the VOC and the gelatin and IL moieties. As a result of the admittance change of the gel, the conductance at a fixed frequency can be measured, and an electrical response is obtained. This process is reversible upon VOC desorption.[26] The six different ionogel compositions were sequentially exposed to a set of VOCs from distinct chemical classes, generating a set of electrical signals characteristic of each ionogel composition—it should be noted that the signals derived from these interactions are a collaborative response of all of the individual components of each formulation. Representative cycles acquired for the tested VOCs on all of the ionogel sensors are presented in Figure 3. All sensor responses were reversible and reproducible upon consecutive exposures, and each VOC yielded typical and different signals (Figure 3). Aliphatic VOCs, such as hexane and heptane, as well as methanol and acetic acid, yielded electrical signals with the lowest amplitudes. Typically, sensors with the highest ionic conductivity values yielded signals with higher amplitudes (Table S1 and Figure 2). After signal

https://doi.org/10.1021/acsmaterialsau.3c00042
ACS Mater. Au XXXX, XXX, XXX−XXX

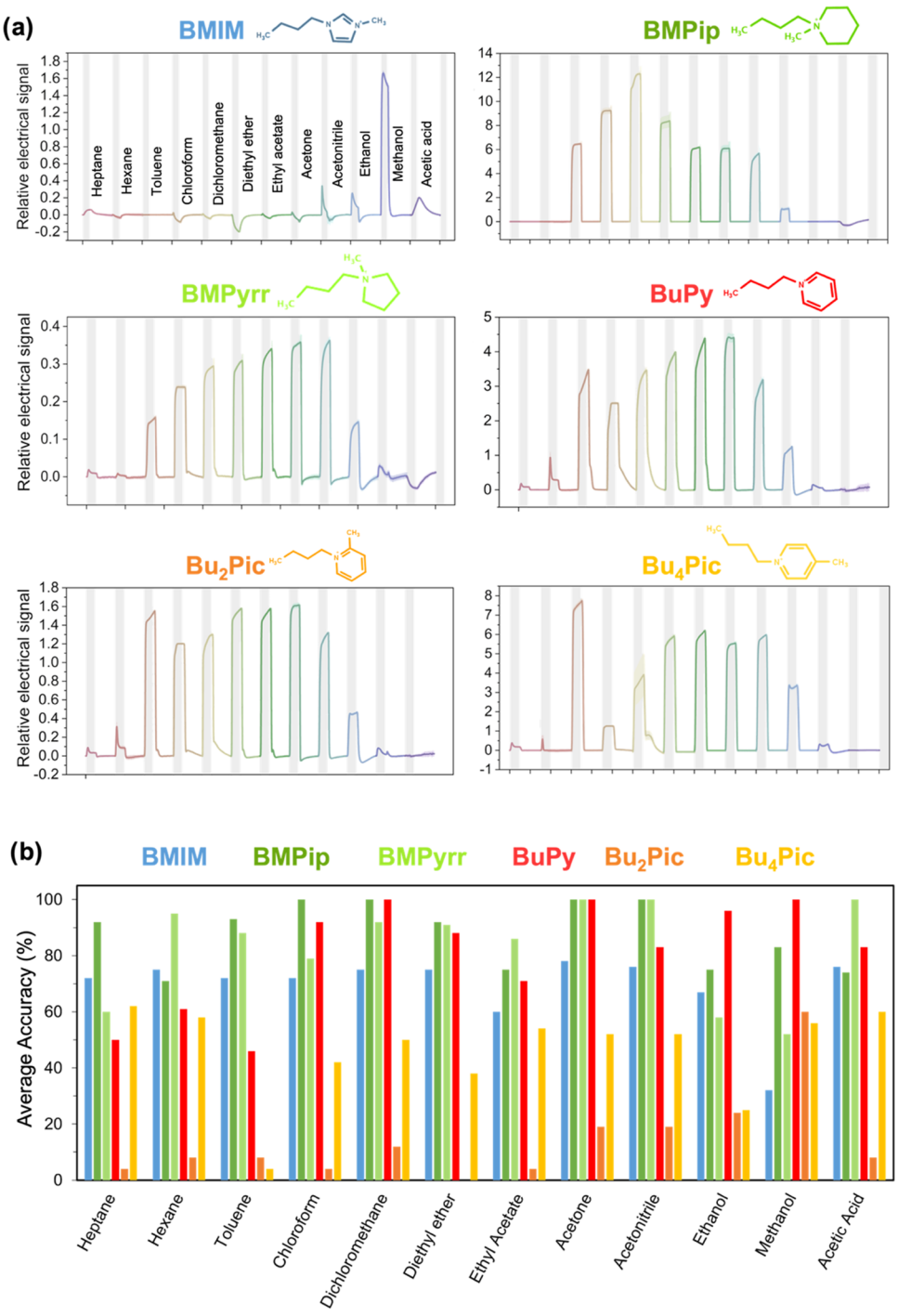

Figure 3. (a) Representative signals of the electrical amplitude responses of all gelatin ionogels to distinct VOCs. Each curve represents the average and standard deviation of at least 19 replicate cycles from the same sensor. VOC exposure periods (5 s) are highlighted in gray, and each cycle corresponds in total to 15 s. The plots were generated by Python. (b) Average accuracy scores from a confusion matrix analysis regarding the ability of each sensor to accurately predict each volatile being tested during the electrical e-nose experiments.

collection, the data were analyzed using machine-learning tools. Morphological features and parameters of curve fitting models[27] were selected and treated by computational methods and used as inputs to train and validate an SVM-based classification algorithm. Through this SVM training method, the algorithm was able to make predictions on unknown inputs. A confusion matrix is generated, representing the accuracy at which every volatile was predicted by each sensor during the experiment; for further detailed studies on the accuracy of performance of the algorithm for each VOC, please see the Supporting Information (Figure S5). To discuss further how accurately the sensors can classify and identify the volatiles, a summarized plot of accuracies (in percentage) is displayed in Figure 3. The highest overall accuracies provided by the ionogel sensors to predict the studied volatiles were registered for BMPip, BMPyrr, and BuPy (88, 83 and 81%, respectively), followed by BMIM (69%), and the lowest ones were observed for Bu_4Pic and Bu_2Pic (46 and 14%,

https://doi.org/10.1021/acsmaterialsau.3c00042
ACS Mater. Au XXXX, XXX, XXX−XXX

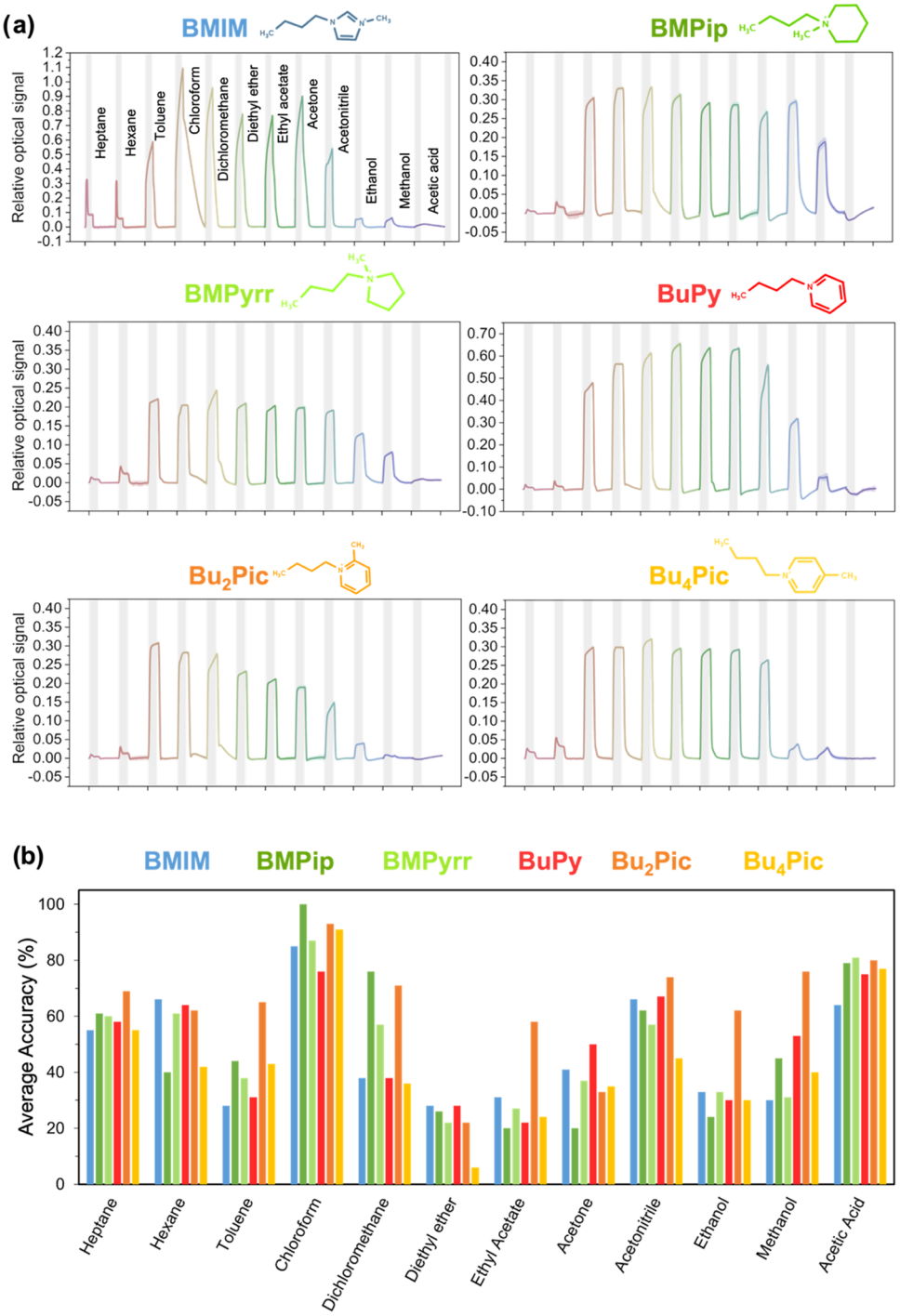

Figure 4. (a) Representative signals of the optical amplitude responses of all hybrid gels to distinct VOCs. Each curve represents the average and standard deviation of at least 19 replicate cycles from the same sensor. VOC exposure periods (5 s) are highlighted in gray, and each cycle corresponds in total to 15 s. The plots were generated by Python. (b) Average accuracy scores from a confusion matrix analysis regarding the ability of each sensor to accurately predict each volatile being tested during the optical e-nose experiments.

respectively), both from the pyridinium family. These global performances are in line with those obtained in other studies reported in the literature using ionomaterials with distinct ionic liquids or polymers.[9,11,12] Also, excellent discrimination of some individual volatiles was achieved with the present materials (e.g., methanol with the BuPy sensor), as seen in Figure 3b, and in the confusion matrices in Figure S5, which could be an advantage for the future tuning of VOC-selective sensing arrays.

Interestingly, the cyclic cation families of ILs (BMPip and BMPyrr) exhibit similar behaviors in predicting VOCs, with high scores of accuracy. BMPip and BMPyrr contain cyclic moieties in their cationic part, and these tend to be more hydrophilic, especially when combined with the presence of the Cl^- anion.[23,28,29] BMIM, BuPy, Bu_2Pic, and Bu_4Pic ILs contain aromatic rings in their cationic part, which confer a more hydrophobic character to the cation. For Bu_2Pic, the methyl group, placed in the ortho position within the cation

https://doi.org/10.1021/acsmaterialsau.3c00042
ACS Mater. Au XXXX, XXX, XXX−XXX

structure,[23] could form a second ring with the 4-carbon side chain, minimizing interactions with VOCs and yielding weaker signals. An exception to this was observed for methanol exposure. According to the literature, the presence of the methyl group within the ortho position affords a more hydrophilic character to the IL,[23] which, along with the small size of the methanol molecule, could explain the gel response.

Hybrid Materials As VOC Optical Sensors

The principle of VOC-analyte detection using liquid crystal-based sensors is that the presence of the analyte influences the self-assembly of LCs, triggering an orientational transition[30−32] or a change in the helical pitch of short-pitch chiral systems[33−35] or even a complete loss of long-range ordering.[14,16,36−38] In the case of hybrid gels, the latter is typically observed as the adsorption of gas analytes onto the hybrid materials triggers a 5CB transition to the isotropic phase. This is a reversible process as 5CB can recover its initial configuration upon removal of the volatile with ambient air, as verified via POM observations.[14,16] In hybrid materials, the observed optical signal is a combined result of the effect of the VOC on the different gel components, namely, the gelatin matrix, the ionic liquid, and the IL−LC droplets.[15]

The optical e-nose is designed to monitor the light transmittance of the hybrid material sensors. Any event disrupting the LC molecular order will alter the light intensity, yielding a variation in the optical signal. These signals are essentially the output voltage of the photodiode that monitors the light exiting the system. Consequently, when the signal amplitude increases corresponding to the VOC exposure period, the brightness of the sensor decreases. The experimental protocol for optical gas sensing was identical to the one followed for the electrical e-nose, and after signal collection, the data were analyzed through the same machine-learning algorithm as explained previously for the electrical e-nose process. Also, similar to what was done for the electrical e-nose process, the sensor materials were stored for 1 day to 1 week before signal acquisition. Overall, all sensor responses were reversible, exhibiting an upward trend upon gas analyte exposure, as well as a faster (<1 s) response profile to the tested volatiles (Figure 4a) when compared to other liquid crystal-based sensing geometries reported in the literature (response times between 1 and 200 s).[23−25,29] The cycle signal shape was stable up to the maximum tested storage time of 1 week. Because of this stability, it was possible to use signals yielded by the hybrid material sensor with different storage times to successfully implement the machine-learning algorithm. The representative cycles regarding the optical signals generated by the hybrid material sensors for the set of 12 tested VOCs can be seen in Figure 4a, and also the overall classification accuracy provided by each hybrid sensor is displayed in Figure 4b. The obtained confusion matrices are displayed in the Supporting Information (Figure S6). As already observed for ionogel-based sensors, the structural differences in ILs lead to distinct properties of hybrid gels, contributing to different discrimination potentials toward various VOCs.

The highest overall accuracy in classifying volatiles (Figures 4b and S6) was registered for the Bu_2Pic sensors, achieving a 63% score of overall accuracy in the discrimination of VOCs, and the lowest accuracy was found for the Bu_4Pic sensor (43%) (Figure S6). In our previous studies, hybrid materials composed of gelatin and 5CB, but with 1-butyl-3-methylimidazolium dicyanamide (BMIM DCA) as the ionic liquid, were also studied and were stable after 2 months of storage, providing a 90% accurate VOC prediction;[27] thus, it is expected that upon a more extensive study, identical performances could be reached with the present materials.

It is interesting to note that the BMPip sensors achieved complete discrimination of chloroform (Figures 4 and S6). In general, hydrophobic VOCs, such as hexane and heptane, are likely to interact mainly with the oil phase formed by LC molecules inside the droplets, which can cause different patterns of response, as seen in all gels (Figure 4). Protic VOCs prone to form hydrogen bonds (such as diethyl ether, methanol, ethanol, and acetic acid) tend to interact both with the IL−LC droplets and the gelatin matrix, yielding more complex and varied signals. Interestingly, some sensors possessing members of the pyridinium family of ILs (e.g., BuPy and Bu_2Pic sensors) presented distinct response signals for both alcohols, ethanol and methanol. The Bu_2Pic sensor presented the best classification for both alcohols compared to the remaining sensors. This could be because it has been shown that the ortho position confers a more hydrophilic character to that specific IL[23] when compared to the meta and para positions of the same aromatic compound.

CONCLUSIONS

Ionic liquids and derived materials present high chemical diversity, which can be explored to yield discrete performances in gas sensing. In this work, we varied the cation group of chloride-based ILs to obtain ionogels and hybrid materials with distinct VOC discrimination potentials. The ionogel and hybrid material compositions are simple to prepare by changing the ionic liquid component, and the resulting sensors can be used either individually or as elements of sensor arrays with cross-reactive but complementary responses. The conductivities of the ionogels prepared and the optical properties of the hybrid gels were adequate for the applications exploited in this work. In the future, further material characterizations should be performed, particularly of mechanical properties, especially if distinct applications are envisioned for the ionogels and hybrid gels.

The different ionogels studied yielded versatile electrical sensors, not only providing a good overall classification of VOCs but also successfully discriminating several volatiles, such as acetic acid (BMPyrr sensors), acetone (BMPip, BMPyrr, and BuPy sensors), acetonitrile (BMPip and BMPyrr sensors), chloroform (BMPip sensors), DCM (BMPip and BuPy sensors), and methanol (BuPy sensors), with 100% accuracy. It is also interesting to note that in all ILs, cations with cyclic moieties (BMPip and BMPyrr) showed similar behaviors in predicting VOCs, with high accuracies and very similar signature responses for hydrophobic, as well as hydrophilic, VOCs. Bu_2Pic ionogel sensors exhibited the weakest overall capacity to discriminate volatiles, whereas the opposite was observed for Bu_2Pic optical sensors, which presented the highest general accuracy to discriminate VOCs in the optical e-nose experiment. This was an exception, as, in general, ionogel-based electrical sensors yielded higher accuracies in VOC classification when compared with optical hybrid sensors (Table 1). This may be related to the fact that in hybrid gels, the mechanism of VOC partitioning and sensing is much more complex and dependent on how VOCs interact with the several compartments created within the material. Thus, different ILs create interfaces at the IL−LC droplets and

https://doi.org/10.1021/acsmaterialsau.3c00042
ACS Mater. Au XXXX, XXX, XXX−XXX

Table 1. Overall VOC Classification Accuracies for Each Ionogel and Hybrid Gel with the Six Different ILs, for Both Electrical and Optical e-Nose Experiments

ionic liquid sensor	overall accuracy in electrical e-nose (%)	overall accuracy in optical e-nose (%)
BMIM	69	47
BMPip	88	49
BMPyrr	83	49
BuPy	81	49
Bu_2Pic	14	63
Bu_4Pic	46	43

influence LC molecule alignment in distinct ways. Our results further strengthen the role of ionic liquids as extremely versatile molecules through which chemical diversity can be translated into functional diversity.

EXPERIMENTAL SECTION

Materials and Reagents

Gelatin from bovine skin (gel strength ≈ 225 g; Bloom, Type B) was purchased from Sigma-Aldrich. The liquid crystal 4-cyano-4′-pentylbiphenyl (5CB) was acquired from TCI Europe, and the ionic liquids 1-butyl-3-methylimidazolium chloride ([BMIM][Cl], >98%), 1-butyl-1-methylpiperidinium chloride ([BMPip][Cl], 99%), 1-butyl-1-methylpyrrolidinium chloride ([BMPyrr][Cl], 99%), 1-butylpyridinium chloride ([BuPy][Cl], 99%), 1-butyl-2-methylpyridinium chloride ([Bu_2Pic][Cl], 99%), and 1-butyl-4-methylpyridinium chloride ([Bu_4Pic][Cl], 99%) were purchased from IoLiTec. Dichloromethane (DCM) and hexane were purchased from VWR. Ethanol and acetic acid (purity 99.8%) were purchased from Sigma-Aldrich. Acetonitrile (purity 99.9%), chloroform, diethyl ether (HPLC grade), ethyl acetate, heptane, methanol (HPLC grade), and toluene were supplied by Fisher Scientific. Acetone (purity 99.5%) was purchased from Honeywell, and isopropanol (purity 99.5%) was from ROTH. MilliQ water was used.

Production of Electrical and Optical Sensors

For the production of ionogels and hybrid materials, the protocol described in previous studies[15,16] was followed. The proportion of each added component was 50−75% (w/w) gelatin, 10−25% (w/w) ionic liquid, 1−5% (w/w) liquid crystal, and 10−20% (w/w) water for the hybrid materials. For the ionogels, the liquid crystal component was removed.

For the production of ionogel sensors, the material was spread onto gold interdigitated electrodes deposited on a glass slide using an automatic film applicator equipped with a heated bed and a quadruplex with a predefined thickness of 15 μm (TQC Sheen).[16] Hybrid gel sensors were prepared by spreading the gel on an untreated glass slide using an automatic film applicator equipped with a heated bed and a quadruplex with a predefined thickness of 30 μm (TQC Sheen). After the production of both ionogels and hybrid materials, the sensors were left to rest for 24 h before use.

Characterization of Electrical and Optical Sensors

The ionic conductivity of the ionogels was determined by electrochemical impedance spectroscopy using a potentiostat Gamry Instruments—Reference 3000 (measurement conditions: frequency range from 100 kHz to 0.1 Hz and Vpp 100mV (AC)), as previously described.[8] The conductivity was calculated according to the equation $\sigma = (1/R) \times (l/A)$, where σ represents the conductivity, R is the resistance, l is the thickness of the sample, and A is the area of the sample. Experimental data were collected in duplicate.

The morphology of the hybrid gels was first assessed after production by polarized optical microscopy (POM) in a Zeiss Axio Observer.Z1/7 microscope equipped with an Axiocam 503 color camera and ZEN 2.3 software for image acquisition and processing. Images were obtained under crossed (at 90°) polarizers, as well as without polarizers (bright-field). The optical textures of the hybrid materials were further monitored over 1 month to assess the stability on storage at ambient conditions. An area of interest was defined in each of the hybrid gels, and POM images using crossed polarizers were obtained immediately after production and then every week. The hybrid materials were also characterized by scanning electron microscopy with a Carl Zeiss AURIGA CrossBeam (FIB-SEM) workstation coupled with energy-dispersive X-ray spectroscopy (EDS). The gels were previously coated with Ir and Au.

VOC Discrimination Using Electrical and Optical e-Nose Devices

Both ionogels and hybrid materials were used as gas sensors in tailor-made e-noses. The electrical and optical e-nose versions have a common design and operation. Detailed information on the e-nose setup has been provided in previous publications[8,11,16] and is schematically shown in Figure S1. In the electrical version, the output of the signal acquisition module is the voltage across each sensor, which is inversely proportional to their conductance. In the optical device, the sensors are placed between crossed polarizers and paired with a light-emitting diode and a photodiode to monitor light transmittance. In both versions, the sensor films are placed in the detection chamber, which has 12 or 6 slots in the electrical and optical e-nose device, respectively. These are then sequentially exposed to vapors of 12 different VOCs in the ascending order of polarity (heptane, hexane, toluene, chloroform, dichloromethane, diethyl ether, ethyl acetate, acetone, acetonitrile, ethanol, methanol, and acetic acid) by placing the solvents in a water bath and heating at 37 °C. For each VOC experiment, the tested films are exposed to analyte vapors for 45 consecutive cycles, each cycle consisting of 5 sec of VOC exposure, followed by 10 sec of recovery with ambient air. For each studied material composition, three batches were produced, and triplicates of each batch were tested to ensure the reproducibility of results. The triplicates were stored for 1 day to 1 week after production at ambient conditions ($T \sim 22$ °C and RH ~ 50%) before being used in the e-noses.

The signals obtained from both electrical and optical e-nose experiments were further processed using data analysis tools based on Python libraries (SciPy, sklearn, and novanistrumentation). Subsequently, feature selection and classification algorithms were implemented using Support Vector Machine (SVM), following the procedures previously detailed,[8,11,15,16,26,27,39] and the classification results for all of the tested sensor formulations are presented in normalized confusion matrices (depicting both correct and incorrect prediction rates) and accuracy plots (presenting only the correct prediction rates).

ASSOCIATED CONTENT

Supporting Information

The Supporting Information is available free of charge at https://pubs.acs.org/doi/10.1021/acsmaterialsau.3c00042.

Schematic representation of the experimental setup for the electrical and optical e-nose devices, properties of ionic liquids used in the study, stability to long-term storage through POM, SEM images, and histograms of droplet diameters for all sensing materials, and classification accuracies for ionogels and hybrid materials (PDF)

AUTHOR INFORMATION

Corresponding Author

Ana Cecília Afonso Roque − *Associate Laboratory i4HB - Institute for Health and Bioeconomy, School of Science and Technology, NOVA University Lisbon, 2829-516 Caparica, Portugal; Applied Molecular Biosciences Unit, Department of Chemistry, School of Science and Technology, NOVA*

https://doi.org/10.1021/acsmaterialsau.3c00042
ACS Mater. Au XXXX, XXX, XXX−XXX

University Lisbon, 2829-516 Caparica, Portugal; orcid.org/0000-0002-4586-3024; Email: cecilia.roque@fct.unl.pt

Authors

Ana Rita Oliveira − *Associate Laboratory i4HB - Institute for Health and Bioeconomy, School of Science and Technology, NOVA University Lisbon, 2829-516 Caparica, Portugal; Applied Molecular Biosciences Unit, Department of Chemistry, School of Science and Technology, NOVA University Lisbon, 2829-516 Caparica, Portugal*

Efthymia Ramou − *Associate Laboratory i4HB - Institute for Health and Bioeconomy, School of Science and Technology, NOVA University Lisbon, 2829-516 Caparica, Portugal; Applied Molecular Biosciences Unit, Department of Chemistry, School of Science and Technology, NOVA University Lisbon, 2829-516 Caparica, Portugal*

Susana I. C. J. Palma − *Associate Laboratory i4HB - Institute for Health and Bioeconomy, School of Science and Technology, NOVA University Lisbon, 2829-516 Caparica, Portugal; Applied Molecular Biosciences Unit, Department of Chemistry, School of Science and Technology, NOVA University Lisbon, 2829-516 Caparica, Portugal;* orcid.org/0000-0002-1851-8110

Carina Esteves − *Associate Laboratory i4HB - Institute for Health and Bioeconomy, School of Science and Technology, NOVA University Lisbon, 2829-516 Caparica, Portugal; Applied Molecular Biosciences Unit, Department of Chemistry, School of Science and Technology, NOVA University Lisbon, 2829-516 Caparica, Portugal*

Arménio Barbosa − *Associate Laboratory i4HB - Institute for Health and Bioeconomy, School of Science and Technology, NOVA University Lisbon, 2829-516 Caparica, Portugal; Applied Molecular Biosciences Unit, Department of Chemistry, School of Science and Technology, NOVA University Lisbon, 2829-516 Caparica, Portugal*

Complete contact information is available at: https://pubs.acs.org/10.1021/acsmaterialsau.3c00042

Author Contributions

A.R.O. contributed to the data analysis, investigation, and writing—original draft; Efthymia Ramou contributed to the review and editing of the original draft (supporting); S.I.J.P. contributed to validation methodology, software, validation, and review; C.E. contributed to validation methodology, and validation; A.J.M.B. contributed to validation methodology and software; A.C.A.R. contributed to supervision and review. All authors have given approval to the final version of the manuscript. CRediT: **Ana Rita Oliveira** formal analysis (lead), investigation (lead), methodology (supporting), writing-original draft (lead); **Efthymia Ramou** writing-original draft (supporting), writing-review & editing (supporting); **Susana I.C.J. Palma** methodology (equal), software (equal), validation (equal), writing-review & editing (supporting); **Carina Esteves** methodology (supporting), validation (supporting); **Arménio Barbosa** software (supporting), validation (supporting); **Ana Cecilia Afonso Roque** funding acquisition (lead), methodology (lead), project administration (lead), supervision (lead), validation (lead), writing-review & editing (lead).

Notes

The authors declare no competing financial interest.

ACKNOWLEDGMENTS

This research was funded by the European Research Council (ERC) under the EU Horizon 2020 research and innovation program [grant reference SCENT-ERC-2014-STG-639123, 2015−2022, and Grant Agreement No. 101069405—ENSURE—ERC-2022-POC1] and by national funds from FCT-Fundação para a Ciência e a Tecnologia, I.P., for projects PTDC/BII-BIO/28878/2017, PTDC/CTM-CTM/3389/2021, UIDP/04378/2020, and UIDB/04378/2020 of the Research Unit on Applied Molecular Biosciences-UCIBIO and the project LA/P/0140/2020 of the Associate Laboratory Institute for Health and Bioeconomy-i4HB. The authors thank FCT/MCTES for the PhD grant SFRH/BD/128687/2017.

ABBREVIATIONS

5CB	4-cyano-4′-pentylbiphenyl
[BMIM][Cl]	1-butyl-3-methylimidazolium chloride
[BMPip][Cl]	1-butyl-1-methylpiperidinium chloride
[BMPyrr][Cl]	1-butyl-1-methylpyrrolidinium chloride
[BuPy][Cl]	1-butylpyridinium chloride
[Bu_2Pic][Cl]	1-butyl-2-methylpyridinium chloride
[Bu_4Pic][Cl]	1-butyl-4-methylpyridinium chloride
e-nose	electronic nose
IL	ionic liquid
LC	liquid crystal
POM	polarized optical microscopy

REFERENCES

(1) Le Bideau, J.; Viau, L.; Vioux, A. Ionogels, Ionic Liquid Based Hybrid Materials. *Chem. Soc. Rev.* **2011**, *40*, 907−925.

(2) Marullo, S.; D'Anna, F. How Ionic Liquid Gels Work on the Removal of Bisphenol A from Wastewater. *ACS Mater. Au* **2023**, *3*, 112−122.

(3) Imam, H. T.; Hill, K.; Reid, A.; Mix, S.; Marr, P. C.; Marr, A. C. Supramolecular Ionic Liquid Gels for Enzyme Entrapment. *ACS Sustainable Chem. Eng.* **2023**, *11*, 6829−6837.

(4) Sun, L.; Huang, H.; Ding, Q.; Guo, Y.; Sun, W.; Wu, Z.; Qin, M.; Guan, Q.; You, Z. Highly Transparent, Stretchable, and Self-Healable Ionogel for Multifunctional Sensors, Triboelectric Nanogenerator, and Wearable Fibrous Electronics. *Adv. Fiber Mater.* **2022**, *4*, 98−107.

(5) Tseng, M. C.; Chu, Y. H. Chemoselective Gas Sensing Ionic Liquids. *Chem. Commun.* **2010**, *46*, 2983−2985.

(6) Chang, A.; Li, H. Y.; Chang, I. N.; Chu, Y. H. Affinity Ionic Liquids for Chemoselective Gas Sensing. *Molecules* **2018**, *23*, 2380.

(7) Chang, Y. P.; Chu, Y. H. Gas Sensing Ionic Liquids on Quartz Crystal Microbalance. In *Progress and Developments in Ionic Liquids*; Handy, S., Ed.; IntechOpen, 2017; pp 35−50.

(8) Esteves, C.; Palma, S. I. C. J.; Costa, H. M. A.; Alves, C.; Santos, G. M. C.; Ramou, E.; Carvalho, A. L.; Alves, V.; Roque, A. C. A. Tackling Humidity with Designer Ionic Liquid-Based Gas Sensing Soft Materials. *Adv. Mater.* **2022**, *34*, No. 2107205.

(9) Gonçalves, W. B.; Cervantes, E. P.; Pádua, A. C. C. S.; Santos, G.; Palma, S. I. C. J.; Li, R. W. C.; Roque, A. C. A.; Gruber, J. Ionogels Based on a Single Ionic Liquid for Electronic Nose Application. *Chemosensors* **2021**, *9*, No. 201.

(10) Esteves, C.; Ramou, E.; Porteira, A. R. P.; Moura Barbosa, A. J.; Roque, A. C. A. Seeing the Unseen: The Role of Liquid Crystals in Gas-Sensing Technologies. *Adv Opt Mater* **2020**, *8*, No. 1902117.

(11) Moreira, I. P.; Esteves, C.; Palma, S. I. C. J.; Ramou, E.; Carvalho, A. L. M.; Roque, A. C. A. Synergy between Silk Fibroin and Ionic Liquids for Active Gas-Sensing Materials. *Mater. Today Bio* **2022**, *15*, No. 100290.

(12) Oliveira, A. R.; Costa, H. M. A.; Ramou, E.; Palma, S. I. C. J.; Roque, A. C. A. Effect of Polymer Hydrophobicity in the Performance of Hybrid Gel Gas Sensors for E-Noses. *Sensors* **2023**, *23*, No. 3531.

(13) Ramou, E.; Palma, S. I. C. J.; Roque, A. C. A. A Room Temperature 9CB-based Chemical Sensor. *Nano Select* (in press). **2023** DOI: 10.1002/nano.202200153.
(14) Ramou, E.; Palma, S. I. C. J.; Roque, A. C. A. Nanoscale Events on Cyanobiphenyl-Based Self-Assembled Droplets Triggered by Gas Analytes. *ACS Appl. Mater. Interfaces* **2022**, *14*, 6261−6273.
(15) Hussain, A.; Semeano, A. T. S.; Palma, S. I. C. J.; Pina, A. S. P.; Almeida, J.; Medrado, B. F. F.; Pádua, A. C. C. S.; Carvalho, A. L.; Dionísio, M.; Li, R. W. C.; Gamboa, H.; Ulijn, R. V.; Gruber, J.; Roque, A. C. A. Tunable Gas Sensing Gels by Cooperative Assembly. *Adv. Funct. Mater.* **2017**, *27*, No. 1700803.
(16) Esteves, C.; Santos, G. M. C.; Alves, C.; Palma, S. I. C. J.; Porteira, A. R.; Filho, J.; Costa, H. M. A.; Alves, V. D.; Morais Faustino, B. M.; Ferreira, I.; Gamboa, H.; Roque, A. C. A. Effect of Film Thickness in Gelatin Hybrid Gels for Artificial Olfaction. *Mater. Today Bio* **2019**, *1*, No. 100002.
(17) Tomé, L. I. N.; Domínguez-Pérez, M.; Cláudio, A. F. M.; Freire, M. G.; Marrucho, I. M.; Cabeza, O.; Coutinho, J. A. P. On the Interactions between Amino Acids and Ionic Liquids in Aqueous Media. *J. Phys. Chem. B* **2009**, *113*, 13971−13979.
(18) Ramou, E.; Rebordão, G.; Palma, S. I. C. J.; Roque, A. C. A. Stable and Oriented Liquid Crystal Droplets Stabilized by Imidazolium Ionic Liquids. *Molecules* **2021**, *26*, 6044.
(19) Covington, J. A.; Marco, S.; Persaud, K. C.; Schiffman, S. S.; Nagle, H. T. Artificial Olfaction in the 21stCentury. *IEEE Sens. J.* **2021**, *21*, 12969−12990.
(20) Stępniak, I.; Andrzejewska, E. Highly Conductive Ionic Liquid Based Ternary Polymer Electrolytes Obtained by in Situ Photopolymerisation. *Electrochim. Acta* **2009**, *54*, 5660−5665.
(21) Andrzejewska, E.; Marcinkowska, A.; Zgrzeba, A. Ionogels - Materials Containing Immobilized Ionic Liquids. *Polimery/Polymers* **2017**, *62*, 344−352.
(22) Bhattacharjee, A.; Carvalho, P. J.; Coutinho, J. A. P. The Effect of the Cation Aromaticity upon the Thermophysical Properties of Piperidinium- and Pyridinium-Based Ionic Liquids. *Fluid Phase Equilib.* **2014**, *375*, 80−88.
(23) Khan, I.; Taha, M.; Pinho, S. P.; Coutinho, J. A. P. Interactions of Pyridinium, Pyrrolidinium or Piperidinium Based Ionic Liquids with Water: Measurements and COSMO-RS Modelling. *Fluid Phase Equilib.* **2016**, *414*, 93−100.
(24) Fernández Requejo, P.; Diaz, I.; Gonzalez, E. J.; Dominguez, A. Mutual Solubility of Aromatic Hydrocarbons in Pyrrolidinium and Ammonium-Based Ionic Liquids and Its Modeling Using the Cubic-Plus-Association (CPA) Equation of State. *J. Chem. Eng. Data* **2017**, *62*, 633−642.
(25) Reichardt, C. Polarity of Ionic Liquids Determined Empirically by Means of Solvatochromic Pyridinium N-Phenolate Betaine Dyes. *Green Chem.* **2005**, *7*, 339−351.
(26) Palma, S. I. C. J.; Esteves, C.; Padua, A. C. C. S.; Alves, C. M.; Santos, G. M. C.; Costa, H. M. A.; Dionisio, M.; Gamboa, H.; Gruber, J.; Roque, A. C. A. In *Enhanced Gas Sensing with Soft Functional Materials*, 2019 IEEE International Symposium on Olfaction and Electronic Nose (ISOEN), IEEE: Fukuoka, Japan, 2019; pp 1−3.
(27) Santos, G.; Alves, C.; Pádua, A.; Palma, S.; Gamboa, H.; Roque, A. In *An Optimized E-Nose for Efficient Volatile Sensing and Discrimination*. Proceedings of the 12th International Joint Conference on Biomedical Engineering Systems and Technologies; Roque, A.; Roque, A.; Fred, A.; Gamboa, H., Eds.; SCITEPRESS - Science and Technology Publications: Prague, Czech Republic, 2019; pp 36−46.
(28) Yaghini, N.; Nordstierna, L.; Martinelli, A. Effect of Water on the Transport Properties of Protic and Aprotic Imidazolium Ionic Liquids-an Analysis of Self-Diffusivity, Conductivity, and Proton Exchange Mechanism. *Phys. Chem. Chem. Phys.* **2014**, *16*, 9266−9275.
(29) Freire, M. G.; Neves, C. M. S. S.; Carvalho, P. J.; Gardas, R. L.; Fernandes, A. M.; Marrucho, I. M.; Santos, L. M. N. B. F.; Coutinho, J. A. P. Mutual Solubilities of Water and Hydrophobic Ionic Liquids. *J. Phys. Chem. B* **2007**, *111*, 13082−13089.
(30) Bedolla Pantoja, M. A.; Abbott, N. L. Surface-Controlled Orientational Transitions in Elastically Strained Films of Liquid Crystal That Are Triggered by Vapors of Toluene. *ACS Appl. Mater. Interfaces* **2016**, *8*, 13114−13122.
(31) Szilvási, T.; Bao, N.; Yu, H.; Twieg, R. J.; Mavrikakis, M.; Abbott, N. L. The Role of Anions in Adsorbate-Induced Anchoring Transitions of Liquid Crystals on Surfaces with Discrete Cation Binding Sites. *Soft Matter* **2018**, *14*, 797−805.
(32) Bi, X.; Yang, K. L. Real-Time Liquid Crystal-Based Glutaraldehyde Sensor. *Sens. Actuators, B* **2008**, *134*, 432−437.
(33) Sutarlie, L.; Qin, H.; Yang, K. L. Polymer Stabilized Cholesteric Liquid Crystal Arrays for Detecting Vaporous Amines. *Analyst* **2010**, *135*, 1691−1696.
(34) Shibaev, P. V.; Carrozzi, D.; Vigilia, L.; DeWeese, H. Liquid Crystal Nose, Chiral Case: Towards Increased Selectivity and Low Detection Limits. *Liq. Cryst.* **2019**, *46*, 1309−1317.
(35) Chang, C. K.; Kuo, H. L.; Tang, K. T.; Chiu, S. W. Optical Detection of Organic Vapors Using Cholesteric Liquid Crystals. *Appl. Phys. Lett.* **2011**, *99*, No. 073504.
(36) Bolleddu, R.; Chakraborty, S.; Bhattacharjee, M.; Bhandaru, N.; Thakur, S.; Gooh-Pattader, P. S.; Mukherjee, R.; Bandyopadhyay, D. Pattern-Directed Phase Transitions and VOC Sensing of Liquid Crystal Films. *Ind. Eng. Chem. Res.* **2020**, *59*, 1902−1913.
(37) Reyes, C. G.; Sharma, A.; Lagerwall, J. P. F. Non-Electronic Gas Sensors from Electrospun Mats of Liquid Crystal Core Fibres for Detecting Volatile Organic Compounds at Room Temperature. *Liq. Cryst.* **2016**, *43*, 1986−2001.
(38) Rodrigues, R.; Palma, S. I. C. J.; Correia, V. G.; Padrao, I.; Pais, J.; Banza, M.; Alves, C.; Deuermeier, J.; Martins, C.; Costa, H. M. A.; Ramou, E.; Silva Pereira, C.; Roque, A. C. A. Sustainable Plant Polyesters as Substrates for Optical Gas Sensors. *Mater. Today Bio* **2020**, *8*, No. 100083.
(39) Oliveira, A. R.; Ramou, E.; Teixeira, D. G.; Palma, S. I. C. J.; Roque, A. C. A. In *Incorporation of VOC-Selective Peptides in Gas Sensing Materials*, Proceedings ofthe 15th International Joint Conference on Biomedical Engineering Systems and Technologies (BIOSTEC 2022); SCITEPRESS, 2022; pp 25−34.

https://doi.org/10.1021/acsmaterialsau.3c00042
ACS Mater. Au XXXX, XXX, XXX−XXX